Delivery of beclomethasone dipropionate nanosuspensions with an electronic cigarette

Luca Casula[1], Chiara Sinico[1], Donatella Valenti[1], Elena Pini[2], Rosa Pireddu[1], Michele Schlich[1,3], Francesco Lai[1*], Anna Maria Fadda[1]

[1]Dipartimento di Scienze della Vita e dell'Ambiente, Sezione di Scienze del Farmaco, CNBS, Università degli Studi di Cagliari, Cagliari, 09124, Italy

[2]DISFARM, Sezione di Chimica Generale e Organica "A. Marchesini", Università degli Studi di Milano, Via Venezian 21, Milano, 20133, Italy

[3]Laboratory of Nanotechnology for Precision Medicine, Istituto Italiano di Tecnologia, Genova, 16163, Italy;

Abstract

The aim of this work was to ascertain the ability of electronic nicotine delivery systems (ENDS) to deliver drug nanocrystals through the produced aerosol. A nanocrystal nanosuspension of beclomethasone dipropionate, a synthetic chlorinated corticosteroid diester commonly used by inhalation in the treatment of asthma and chronic obstructive pulmonary disease, was prepared with a wet media milling technique using Poloxamer 188 as stabilizer. The obtained nanosuspension was thoroughly characterized by different techniques: transmission electron microscopy, photon correlation spectroscopy, X-ray powder diffractometry and Fourier transform infrared spectroscopy. The nanosuspension was then loaded in the cartomizer of the electronic cigarette and the produced aerosol was collected and analysed, confirming the presence of drug nanocrystals. The results of this study suggested the possible alternative use of ENDS as medical device for the delivery of poorly soluble drugs.

Keywords: nanocrystals; electronic cigarette; nanosuspension; beclomethasone dipropionate; pulmonary delivery; ENDS

*Correspondence: frlai@unica.it

1. Introduction

Electronic nicotine delivery systems (ENDS) – commonly called electronic cigarettes, or E-cigarettes – are marketed as aerosol producing devices for the delivery of tobacco-free nicotine, usually in propylene glycol or glycerine solutions. The main components are an aerosol generator with a heating element ('atomiser'), a liquid storage area ('cartridge'), a flow sensor (in some devices), and a re-chargeable battery. Atomizer and cartridge are often combined together to form a 'cartomizer'(Trtchounian et al., 2010). Since e-cigarettes were developed with the aim of mimicking the action of smoking, their design and the vapour production remind of traditional cigarettes. In order to activate the heating element, the button placed on the surface of the atomiser has to be pressed. The aerosol is then produced from the liquid in the cartridge (e-liquid) and delivered upon inhalation. The E-liquid can be easily refilled after consumption, and its composition can slightly differ on the propylene glycol-glycerine ratio. (Brown and Cheng, 2014).

Since tobacco smoke or combustion are not involved, e-cigarettes appear to be safer than conventional cigarettes. However, various toxic and carcinogenic substances have been found in ENDS vapours and components (Cheng, 2014). In particular, metal and silicate particles – including nanoparticles – have been found in cartomizer fluid and aerosol produced by some e-cigarettes made of low-quality materials. Diameter of these nanoparticles was in the range of 10-1000 nm, showing the ability of the e-cigarette aerosol to deliver nanosized material (Williams et al., 2013). Nevertheless, the level of carcinogen biomarkers and toxicants has been proven to be lower when switching from conventional cigarette to e-cigarette (Goniewicz et al., 2018, 2017; Round et al., 2019).

The Tobacco Products Directive 2014/40/EU (TPD) introduced new rules for nicotine-containing electronic cigarettes and became applicable in EU countries in May 2016. However, the TDP does not apply to those e-cigarettes and refill liquids that are authorised as medicines, including nicotine-free vaping devices (European Parliament and the Council of the European Union, 2014). In fact, there has been an increasing interest in the scientific community in the alternative applications of ENDS to deliver different substances. At first, illegal drug vaping has been widely reported (Breitbarth et al., 2018; Varlet, 2016). Afterwards, various studies focused on cannabis delivery – cannavaping – have been carried out (Giroud et al., 2015; Miliano et al., 2020; Nguyen et al., 2016; Varlet et al., 2016). These studies highlighted the versatility of this device and its possible use for therapeutic purposes. Purchez et al. studied the ability of a high-power ENDS to deliver bronchodilators for pulmonary disease treatment. Their

results showed the capacity of the device to generate submicron carrier-droplets containing drug molecules dissolved in the e-liquid (Pourchez et al., 2017). In all these studies, the delivered drugs are soluble in the e-liquid. However, most of the newly developed drugs are poorly hydrosoluble and their bioavailability is limited by their slow dissolution rate. Therefore, their formulation is still challenging, and research has been testing several new approaches and alternative administration routes. Drug nanonization or the use of nanocarriers have already shown their potential in improving bioavailability of drugs classified in class II and class IV of the Biopharmaceutics Classification System (BCS), whose principles can partly be transposed on pulmonary-delivered drugs, taking into consideration the effect of the complex physiology of the respiratory system (Cho et al., 2012; Wauthoz and Amighi, 2015). Therefore, it is worthy of investigation the capability of ENDS to deliver nanoparticles, i.e., both drug nanocrystals and drug loaded nanocarriers. Nanocrystals are nanoparticles of pure drug without any matrix material with an average diameter below 1 μm (typically in the range of 200-500 nm). The drug nanocrystals can be suspended in an outer liquid phase, usually composed of water and/or water-miscible solvents and stabilized using an ionic or non-ionic surfactant or polymers, to obtain a nanosuspension. The reduction of the drug crystal mean diameter below 1 μm dramatically increases the particle surface area and decreases the diffusion layer thickness if compared to coarse and micronized drug, as described by the Prandtl equation, thus, speeding up the dissolution rate (Mosharraf and Nyström, 1995). In addition, nanocrystals are characterized by an enhanced saturation solubility, according to the Freundlich– Ostwald equation (Müller and Peters, 1998). Moreover, nanosuspensions have shown to be suitable to formulate poorly soluble drugs for lung delivery and to have superior pharmacokinetics properties when compared to solutions or coarse suspensions of the same drug (Britland et al., 2012; Chiang et al., 2009; Jacobs and Müller, 2002; Van Eerdenbrugh et al., 2008; Yang et al., 2008; Zhang and Zhang, 2016).

Since the presence of metal and silicate (nano)particles in the aerosol produced by e-cigarettes has been demonstrated, the aim of the present work was to investigate the ability of the ENDS-aerosol to deliver nanocrystals of poorly water-soluble drugs. Beclomethasone dipropionate (BDP) was chosen as a model drug for its well-known effect on the treatment of asthma and chronic obstructive pulmonary disease (COPD) (De Coster et al., 2013; Dompeling et al., 1992; Wood and Barnes, 1995).

BDP nanosuspensions were prepared by a top down - media milling method. Characterization of the nanosuspensions was carried out via different techniques: Dynamic Light Scattering

(DLS), transmission electron microscopy (TEM), differential scanning calorimetry (DSC), X-ray powder diffractometry (XRPD) and Fourier transform infrared (FTIR) spectroscopy. In addition, solubility studies and vaping tests were performed.

To the best of our knowledge, this is the first paper aimed at studying the ability of ENDS to deliver drug nanocrystals, and thus the possibility of using it as alternative inhaler device for nanosized formulations.

2. Materials and Methods

2.1. Materials

Beclomethasone dipropionate and Kolliphor P188 (Poloxamer 188, P188) were obtained from Sigma Aldrich (Italy). Vegetable glycerol and propylene glycol were purchased from Galeno srl (Italy). All the other products were of analytical grade.

2.2. Preparation of BDP nanosuspension

The nanosuspensions were prepared using a wet ball media milling technique. BDP was dispersed in a Poloxamer 188 (P188) water solution using an Ultra Turrax T25 basic for 6 min at 8000 rpm. Nanosuspensions were prepared using a 2:1 (w/w) BDP:P188 ratio. This coarse suspension was divided in 1.5 ml conical microtubes containing about 0.4 g of 0.1-0.2 mm yttrium-stabilized zirconia-silica beads (Silibeads® Typ ZY Sigmund Lindner, Germany). The microtubes were oscillated at 3000 rpm for 150 minutes using a beads-milling cell disruptor equipment (Disruptor Genie®, Scientific Industries, USA). The obtained nanosuspensions of each microtubes were gathered and then separated from the milling beads by sieving. In the preliminary studies, the nanosuspensions were prepared directly in the conical microtubes, without any preliminary homogenisation with the Ultra Turrax, in order to evaluate the optimum milling time. The formulation had a final concentration of 1% BDP and 0.5% P188.

2.3. Particle size analysis

Average diameter and polydispersity index (PDI, as a measure of the size distribution width) of the samples were determined by Dynamic Light Scattering (DLS) using a Zetasizer nano (Malvern Instrument, Worcestershire, United Kingdom). Samples were backscattered by a helium–neon laser (633 nm) at an angle of 173° and a constant temperature of 25°C. Zeta

potential was estimated using the Zetasizer nano by means of the M3-PALS (Phase Analysis Light Scattering) technique. Just before the analysis, nanosuspensions were diluted with distilled water. Furthermore, a medium-term stability study of the BDP nanosuspension stored at room temperature was performed by monitoring average size, polydispersity index, and zeta potential for 30 days. The nanosuspensions were visually inspected before every DLS measurement to check the absence of large precipitated aggregates or phase separation. All the measurements were made in triplicate.

2.4.Lyophilization of BDP nanosuspension

BDP nanosuspensions (1 mL samples) were frozen at -80 °C and then freeze dried for 24 h at -86 °C and 0 mmTorr, using an FDU-8606 Freeze Dryer (Operon Co, Korea).

2.5.Preparation of Poloxamer 188/BDP physical mixture

Drug physical mixtures were prepared by blending Poloxamer 188/BDP in an agata mortar until a homogeneous mixture was obtained. The same ratio of drug/surfactant (2:1, w/w) of the nanosuspension was used.

2.6.Solubility studies

BDP solubility in a home-made e-cigarette liquid (water:vegetable glycerol:propylene glycol=20:40:40 w/w) was measured for the BDP bulk, freeze dried BDP nanocrystals and the Poloxamer 188/BDP physical mixture. The formulations (n = 3) were kept under constant stirring for 48 h at room temperature. Samples were withdrawn and centrifuged at 12,000 rpm for 60 min; the supernatant was centrifuged again at 12,000 rpm for 60 min. Then, 0.2 ml of the clear supernatant were diluted with methanol and analysed by HPLC for BDP content.

2.7.HPLC analysis

Quantitative determination of BDP was performed by HPLC using a liquid chromatograph Alliance 2690 (Waters Corp, Milford, MA) equipped with a photodiode array detector and a computer integrating apparatus (Empower 3). Analyses were performed at 240 nm with a X-Select C18 column (3.5 µm, 4.6 mm × 100 mm, Waters). The mobile phase was a mixture of acetonitrile, water and acetic acid (68.45:31.5:0.05, v/v), delivered at a flow rate of 1 mL/min. Samples (10µL) were injected using an auto sampler. The stock standard solution of BDP was prepared by dissolving the drug in methanol and stored at 4 °C. A standard calibration curve (peak area of BDP vs. known drug concentration) was built up by using standard solutions

prepared by dilution of the stock standard solution with the mobile phase. Calibration graphs were plotted according to the linear regression analysis, which gave a correlation coefficient value (R2) of 0.999. The BDP retention time was 4.15 min. The limit of detection was 0.5 ng while the limit of quantification was 2 ng. Sample preparation and analyses were performed at room temperature.

2.8.Preparation of the e-vaping liquid.

Freeze-dried BDP nanocrystals were dispersed in 200 µL of water, vortexed and made up to 1 mL with a previously prepared solution of vegetable glycerol:propylene glycol (50:50 (w/w)). The final composition of the obtained e-liquid was water:vegetable glycerol:propylene glycol=20:40:40 (w/w). The same procedure was used in case of the vaping tests performed with BDP coarse powder, instead of freeze-dried BDP nanocrystals.

2.9.E-cigarette vaping test

The e-vaping liquid was loaded in the SMOK® QBOX (SmokTech, China) e-cigarette, equipped with a V8-Baby M2 0.25 Ω Dual Coil. The device was fully charged before every vaping test, and the battery level was never lower than 50% during the experiments. A syringe was connected to the atomizer through a plastic tube. The simultaneous activation of the e-cigarette and the retraction of the plunger led to the production of aerosol, which was gradually expelled in a vial immersed in an ice bath for the condensation of the aerosol. The aerosol production was carried out according to the following parameters: 60 mL syringe, 4.0 ± 0.3 seconds-puff, interpuff pause of 30 seconds. The obtained samples were analysed by TEM, DLS and HPLC.

2.10. Transmission electron microscopy

BDP coarse powder, freshly prepared nanosuspensions and condensed aerosol were analysed through transmission electron microscopy (TEM) in order to investigate the presence of crystals and their morphology. After depositing on carbon-coated copper grids (200 mesh), drug crystals were viewed using a JEOL JEM 1400 Plus (CeSAR, Centro Servizi d'Ateneo per la Ricerca, University of Cagliari), with an accelerating voltage of 120 kV in Bright-field mode.

2.11. X-ray powder diffractometry

BDP raw powder, P188 raw powder, physical mixture of P188 and BDP and freeze-dried BDP nanocrystals were investigated by X-ray Powder Diffraction (XRPD). The XRPD patterns were

collected with a Rigaku MiniFlex diffractometer, operating at 30 kV and at 15 mA, using, the Cu Kα line at 1.54056 Å as radiation source. Each sample was analysed from 3 to 60 2θ, in steps of 0.02, using a scan step time of 2.00 seconds. The results were then obtained as peak height (intensity) versus 2θ.

2.12. Fourier transform infrared spectroscopy (FTIR)

FT-IR spectra of BDP raw powder, P188 raw powder, physical mixture of P188 and BDP and freeze-dried BDP nanocrystals were collected using the Spectrum One Perkin Elmer (MA, USA) FT-IR Spectrometer in the spectral region between 4000 and 600 cm-1, and analyzed by transmittance technique with 32 scans and 4 cm-1 resolution. Samples were mixed in a mortar with KBr (1:100) and pressed by a hydraulic press (10 tons) into small tablets.

3. Results and discussion

3.1. Preparation and characterization of BDP nanosuspension

BDP nanosuspension were successfully prepared through a wet media milling technique. P188 - chosen as stabilizer - is a non-ionic linear low toxic copolymer, which is used in many commercially available products (Moloughney and Weisleder, 2013). The average diameter and PDI modifications as a function of milling time were preliminarily studied (Figure 1).

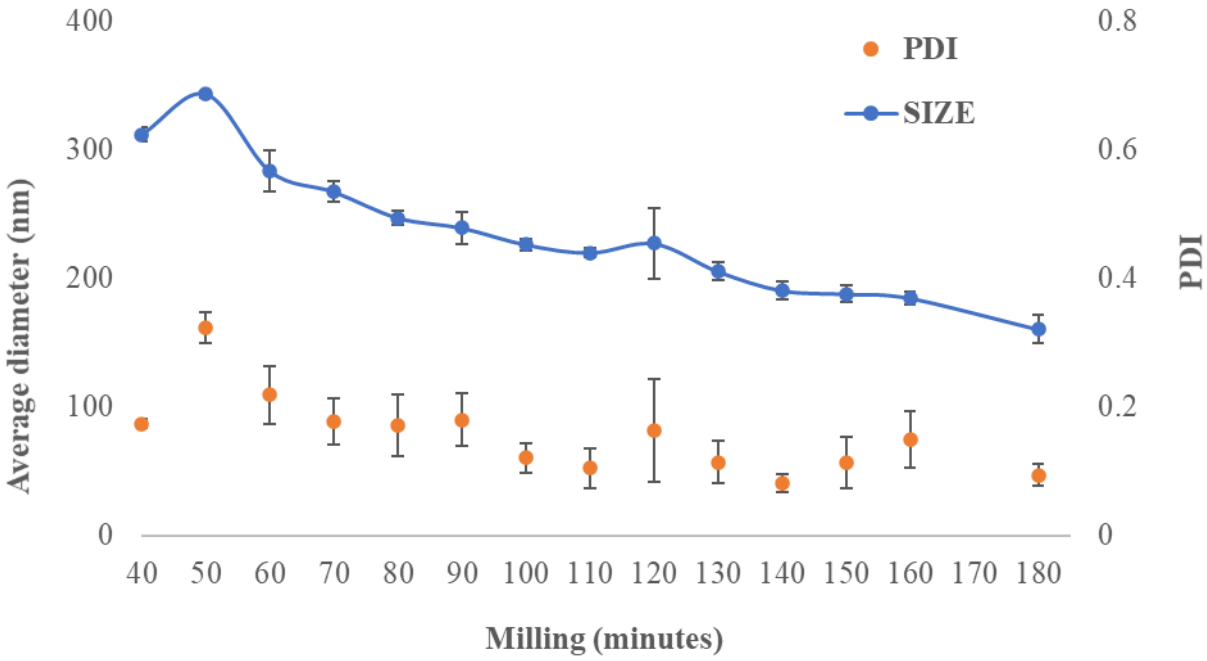

Figure 1. Milling process optimization of BDP nanosuspension as a function of minutes of milling, measured using DLS (average diameter and PDI, mean ± SD; n=3).

In the first 10 cycles (corresponding to 100 minutes of milling), a significant decrease of the mean particle size and PDI was observed. The particle sized reduction slowed down during the last cycles, leading to a final average diameter of approximately 161 nm and a PDI of 0.09 at 180 minutes of milling. In light of these results, we decided to prepare nanosuspensions using a preliminary homogenization with the Ultra Turrax, followed by 150 minutes of milling corresponding to 15 cycles. The composition and physico-chemical data relative to the lead formulation are presented in Table 1. The chosen protocol led to an average diameter of approximately 168 and a PDI of 0.09.

Table 1. Average diameter, polydispersity index (PDI) and Zeta potential of freshly prepared BDP nanosuspension.

Active ingredient	Stabilizer	Properties		
		Average diameter (nm)	PDI	Zeta potential (mV)
BDP 1% (w/w)	P188 0.5% (w/w)	168 ± 5	0.090 ±0.048	-25.65 ± 2.33

Average size, PDI and Zeta-potential were evaluated over a period of 30 days, for a medium-term stability study (Figure 2). As it can be seen in the graphs, an increase in size of ~30% was observed during the 30 days of storage. However, a low mean diameter (229 nm) and low PDI

(0.261) were maintained, indicating a fairly narrow size distribution (Patravale et al., 2004). The zeta potential value was highly negative at the end of the stability test (-27.4 mV).

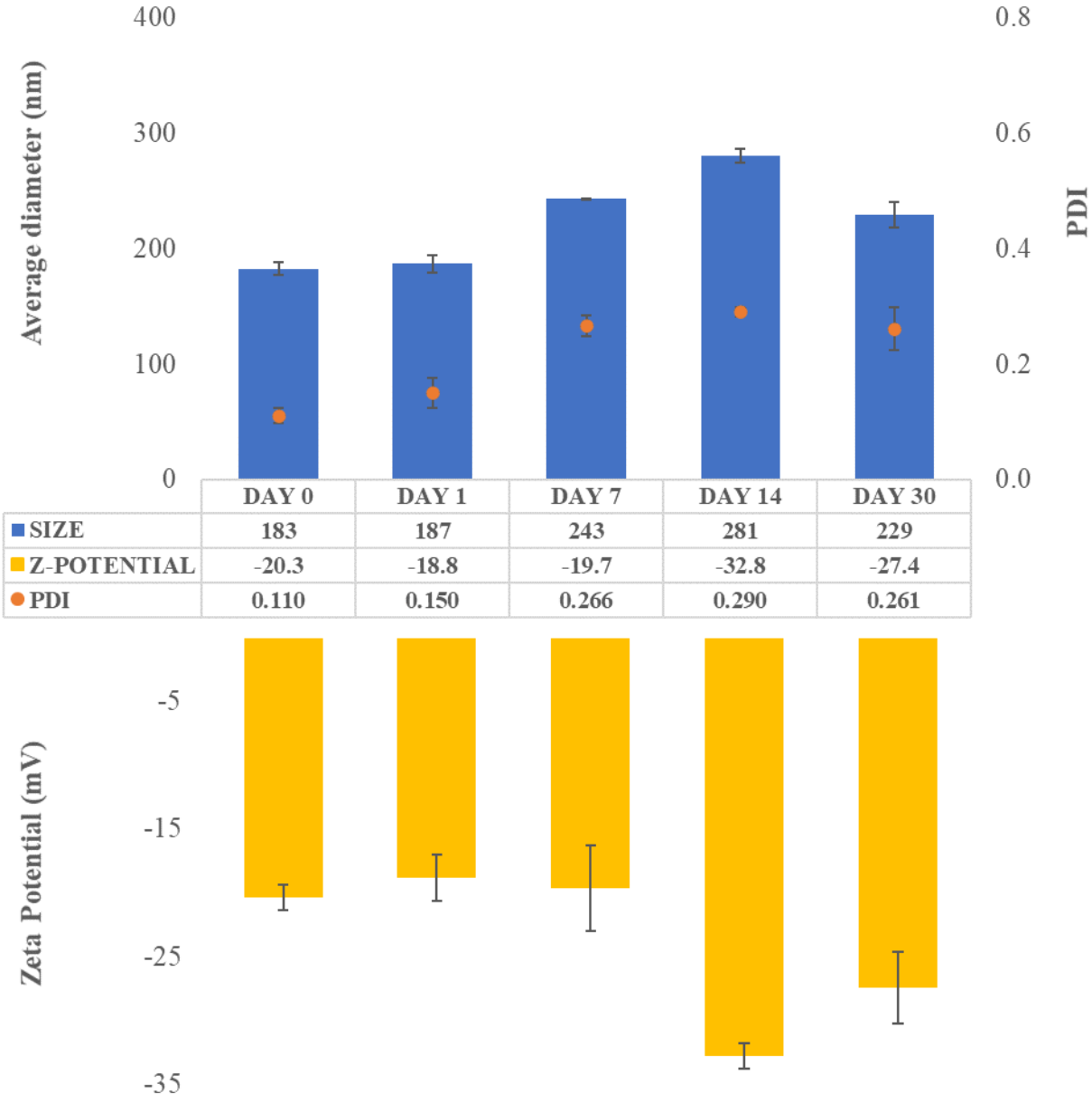

Figure 2. Average diameter (nm), Zeta Potential (mV) and polydispersity index (PDI) of BDP nanosuspension over 30 days of storage at room temperature. Values are presented as mean values ± standard deviation (n = 3).

The morphological changes of BDP crystals after the milling process were evaluated by TEM imaging (Figure 3).

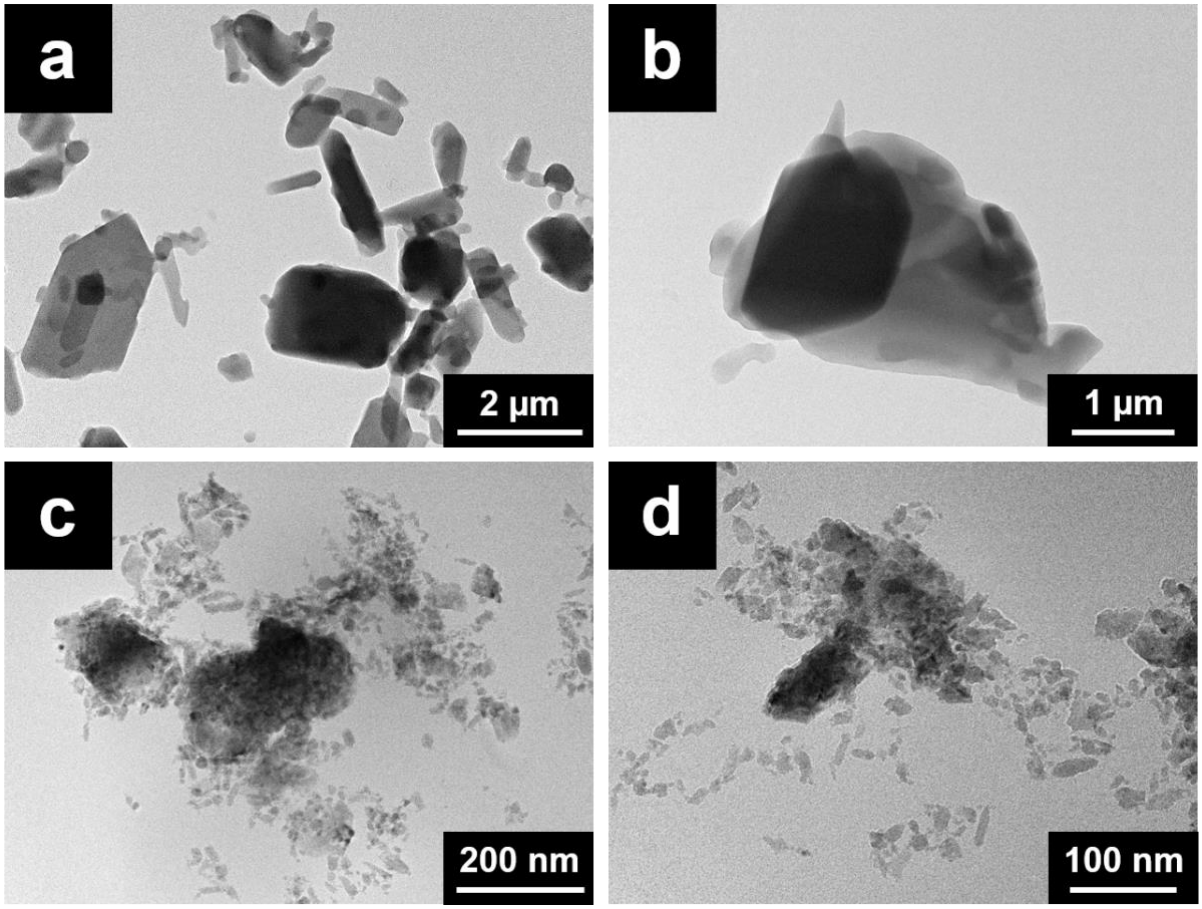

Figure 3. TEM micrographs of BDP raw powder (a-b) and BDP aqueous nanosuspension (c-d).

As can be seen in the TEM micrographs, the milling process modified both the shape and size of BDP crystals. In fact, the high shear forces generated during the process by the collision of the drug crystals and the milling beads – and of the drug crystals themselves – provide the appropriate energy to reduce their size below one micron. BDP nanocrystals (Figure 3c-d) presented a regular and elongated shape, with a homogenous particle size distribution, in accordance with DLS analysis.

As can be seen by the scale bar of the nanosuspension micrographs (Figure 3c-d), the nanocrystals diameter is lower than the value obtained by DLS analysis. This result is in accordance with the literature data (Hinterwirth et al., 2013; Lee et al., 2013; Pabisch et al., 2012; Unsoy et al., 2012), and can be explained by the ability of DLS to measure the hydrodynamic diameter of hydrated particles which is also influenced by all substances adsorbed on the surface of the nanocrystals (hydration layer, polymer shell or surfactants). Thus, it always results larger than the dry particle diameter obtained with TEM or SEM, that measure the geometrical size (Tomaszewska et al., 2013; Tscharnuter, 2006).

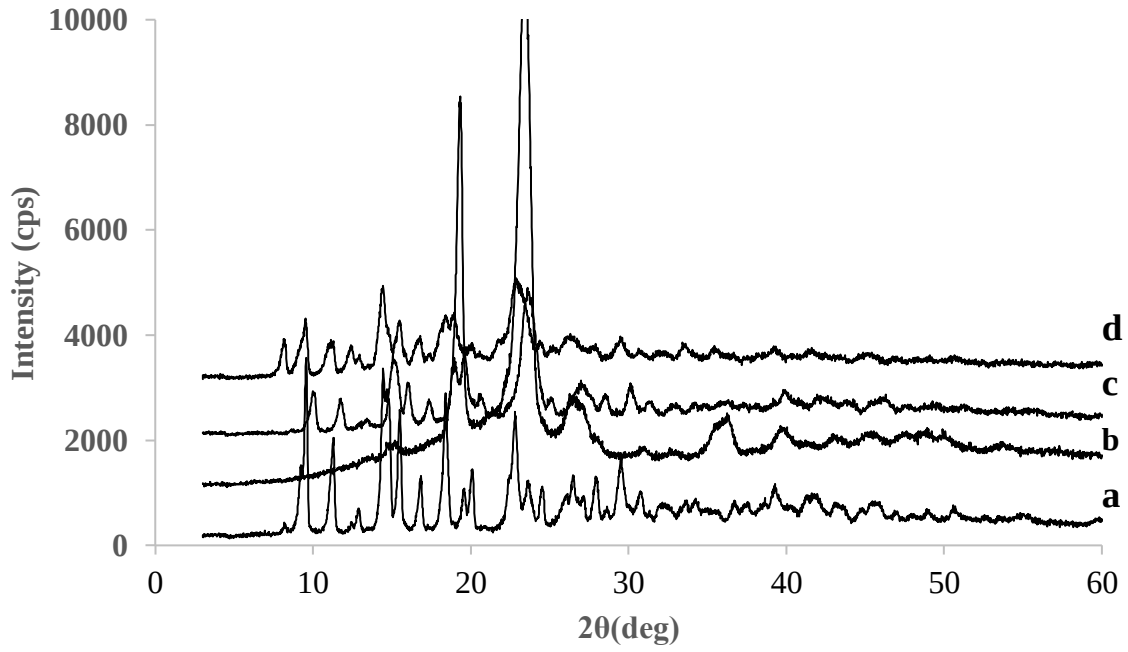

Figure 4 . XRPD analysis of BDP raw powder (a), P188 raw powder (b), physical mixture of P188 and BDP (c) and freeze-dried BDP nanocrystals (d).

XRPD analysis was used to assess the crystallinity of the samples. Commercial BDP showed a crystalline profile with a low intensity signal at 8.5 2θ (deg), absent in the physical mixture, which increased in the NS diffractogram confirming the BDP hydration. However, NS analysis evidenced the presence of the signal at 18.4 2θ (Figure 4d), characteristic of the anhydrous BDP (Wang et al., 2007), suggesting the presence of anhydrous and hydrated BDP in the formulation. Physical mixture and NS still maintained the crystalline profile.

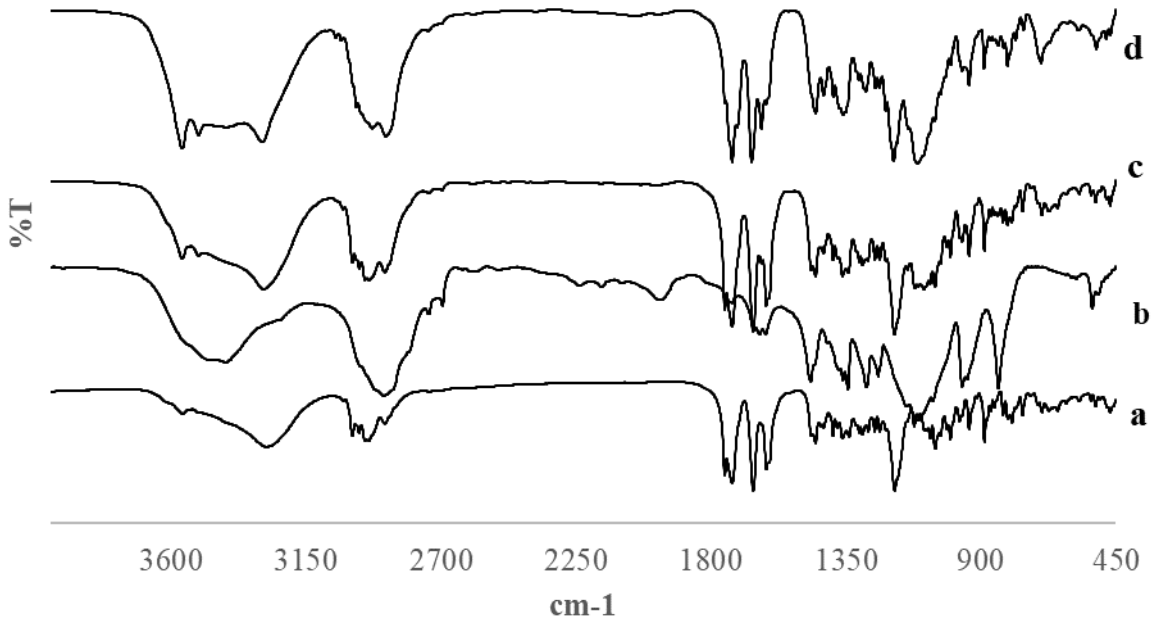

Figure 5. FT-IR analysis of BDP raw powder (a), P188 raw powder (b), physical mixture of P188 and BDP (c) and freeze-dried BDP nanocrystals (d).

The infrared spectrum (Figure 5) of commercial BDP shows the broad O-H stretching at 3562 cm^{-1}, the sharp peak of ester carbonyl group at 1754 cm^{-1}, at 1729 and 1659 cm^{-1} the bands of the conjugated and non-conjugated carbonyl groups, respectively, at 1615 cm^{-1} the carbon double bond stretching, and at 1187 cm^{-1} the C-O peak. The physical mixture spectrum contains the superimposed spectra of each component, in fact in addition to BDP bands, some typical P188 signals due to CH_2 bending (1466 cm^{-1}), in plane O-H bending (1343 cm^{-1}) and C-O stretchings (1112-1108 cm^{-1}) are recognizable. These results suggest that there are no interactions between them. However, the nanosuspension infrared spectrum evidenced the hydration of BDP. In fact, according with literature data for BDP solvates (Weiss et al., 2018), NS spectrum exhibited a large decrease in intensity of BDP C=O (ester) band at 1753 cm^{-1}, the shift of the carbonyl bands at 1665 and 1631 cm^{-1}, and the appearance of a peak at 1712 cm^{-1} due to hydrogen bonding between the hydroxyl hydrogen of water and the carbonyl groups of the BDP moiety. Furthermore, peaks attributable to water hydroxyl groups appeared at 3562 and 3508 cm^{-1}.

The saturation solubility of the freeze-dried nanocrystals, the BDP bulk powder and the Poloxamer 188/BDP physical mixture was measured at 25°C in the home-made e-liquid

(water:glycerol:propylene glycol). The physical mixture was prepared maintaining the same surfactant:drug ratio (1:2, w:w).

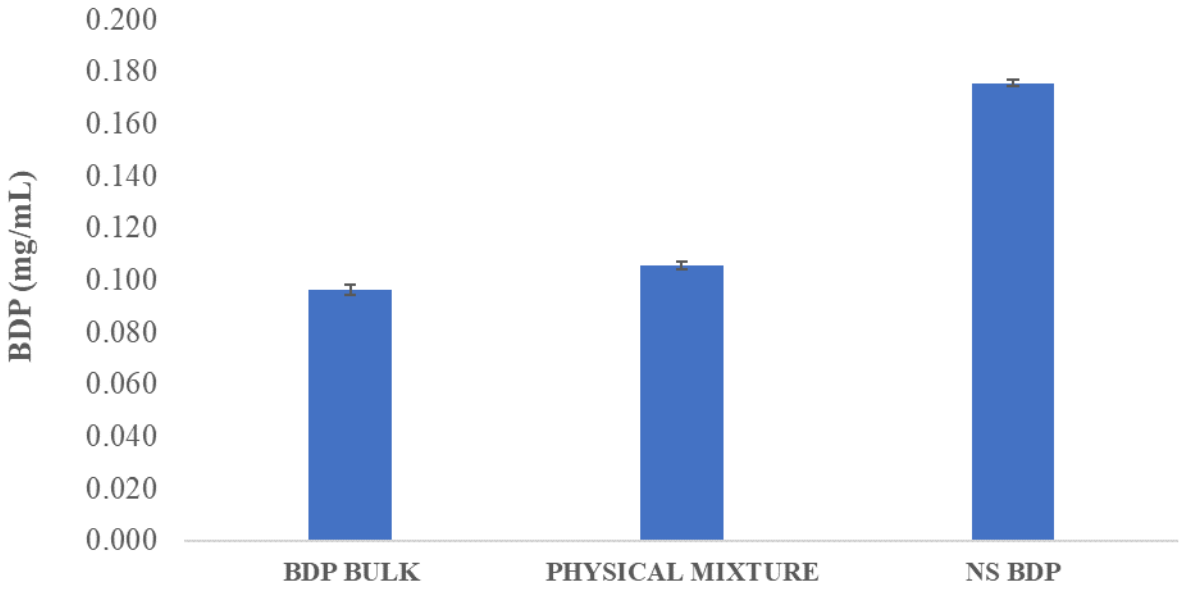

Figure 6. Saturation solubility (mg/mL) of the BDP bulk powder (BDP BULK), physical mixture of P188 and BDP (PHYSICAL MIXTURE) and freeze-dried BDP nanocrystals (NS BDP) in the e-liquid; (mean ± SD, n = 3).

As shown in the Figure 6, the solubility of BDP was found to be 96.33 ± 1.80 µg/mL for the bulk powder drug, which slightly increased to 105.73 ± 1.36 µg/mL with the addition of the surfactant P188 (physical mixture). However, the formation of nanocrystals led to an increase of approximately 80% of the bulk powder solubility, reaching a value of 175.67 ± 1.11 µg/mL. Therefore, these results are in accordance with the Freundlich-Ostwald equation and the drug solubility is enhanced not only by the action of the surfactant, but also by the nanosizing of the particles (Müller and Peters, 1998).

3.2.E-Cigarette vaping test

BDP nanosuspensions were frozen and then freeze-dried for 24 hours. The obtained nanocrystals were resuspended in the vehicle (water, glycerol and propylene glycol) to prepare the *nanosuspensions-containing E-liquid*, which was analysed through DLS and TEM, in order to verify if the properties of the nanocrystals had changed.

As shown in the Table 2, the average diameter of the nanocrystals slightly increased after lyophilization and dispersion in the vehicle. This can be correlated, not only to the different

nature of the vehicle – only water in the first case, water:glycerol:propylene glycol in the second one – but also to the lyophilization process itself, that might modify the morphology of the nanocrystals and promote nanocrystal aggregation. The *nanosuspensions-containing E-liquid* was then loaded in the SMOK® QBOX (SmokTech, China) e-cigarette and the vaping act was simulated. The analysis of the condensed vapour obtained by the test with DLS revealed the presence of nanoparticles – supposedly BDP nanocrystals – with an average diameter of 210 nm, a value comparable to the mean diameter of the freeze-dried nanocrystals dispersed in the vehicle (230 nm). However, the PDI value of the nanoparticles found in the condensed vapour (0.187) was smaller than that of the freeze-dried nanocrystals in the vehicle 0.234. This behaviour could be explained by the ability of the vapour to transport preferably the smallest nanocrystals, thus decreasing the width of the dimensional population (the PDI value). Furthermore, the high temperature reached in the E-cigarette might lead to a partial fusion of the BDP nanoparticles followed by a re-crystallisation in crystals with a smaller diameter.

Table 2. Average diameter, polydispersity index (PDI) of freshly prepared BDP nanosuspension, freeze-dried BDP nanocrystals dispersed in the E-cigarette liquid and BDP nanocrystals in the condensed aerosol of the vaping test; (n=3).

	Average diameter (nm)	PDI
Freshly prepared nanosuspensions	165 ± 4	0.125 ±0.037
Freeze-dried Nanocrystals dispersed in the E-liquid	231 ± 1	0.234 ±0.019
Nanocrystals in the condensed aerosol	211 ± 4	0.187 ±0.020

The *nanosuspensions-containing E-liquid* and the condensed aerosol of the vaping test were studied through TEM analysis. As shown in the micrographs, the morphology of the nanocrystals in the E-liquid (Figure 7a-b) slightly changed if compared to the starting nanosuspensions prepared in water (Figure 3c-d). Moreover, the presence of the nanocrystals in the condensed vapours was revealed by the TEM images, confirming the ability of the E-cigarette to transport the nanoparticles.

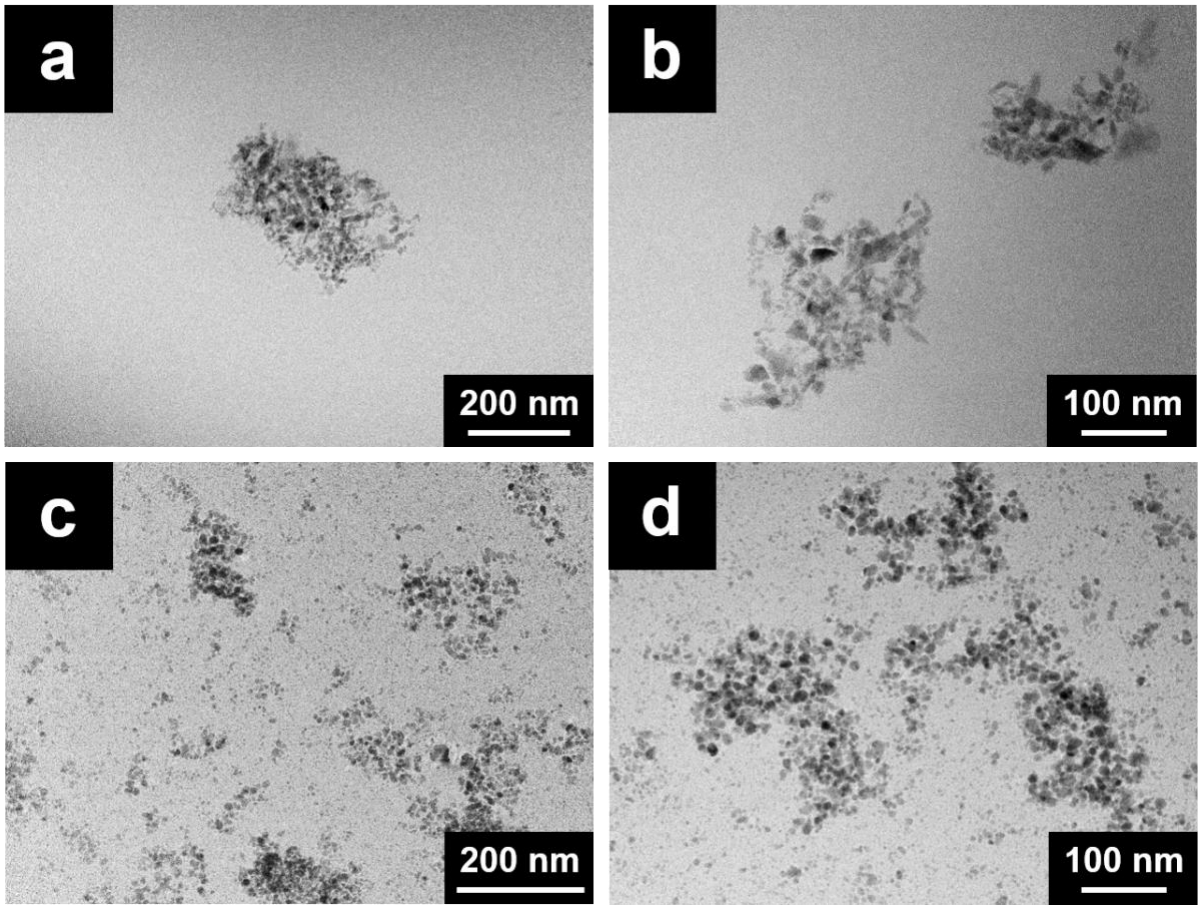

Figure 7. TEM micrographs of freeze-dried BDP nanocrystal dispersed in the e-liquid (a-b) and nanocrystals found in the condensed aerosol of the vaping test (c-d).

In order to verify the hypothesis of the BDP nature of these nanocrystals, the collected samples were diluted with methanol and the obtained solutions were analysed through HPLC. The obtained chromatogram showed the characteristic peak of the drug, eluting at 4.15 min and absorbing at 240 nm.

BDP raw powder was also dispersed in the E-cigarette vehicle and the obtained E-liquid was used for further vaping tests.

The total drug amount (BDP in solution and the suspended (nano)crystals) in the condensed aerosol obtained by vaping E-liquid containing freeze-dried BDP nanosuspensions or BDP raw powder was compared to their solubility values (Figure 8).

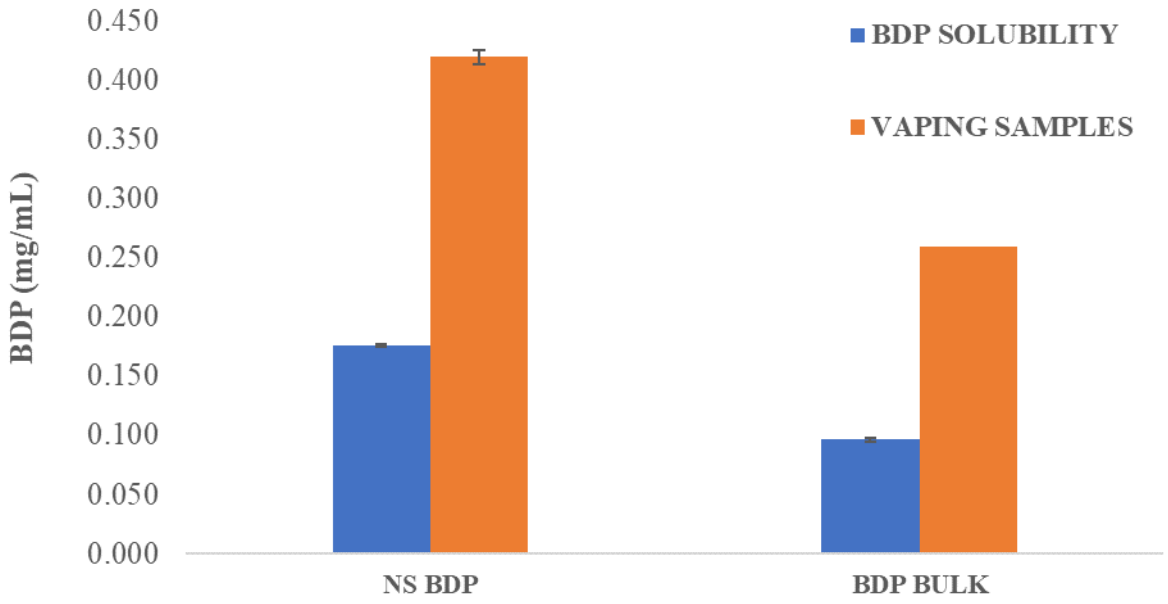

Figure 8. Comparison between BDP solubility values and total BDP amount in the condensed vapour obtained vaping E-liquid containing BDP raw powder (right) or BDP nanosuspensions (left); (n=3).

As shown in the Figure 8, for both nanocrystals and bulk BDP crystals, the total drug amount (BDP in solution and suspended nanocrystals or bulk crystal) in the condensed aerosol is more than two-fold higher than its solubility value at 25°C. This might be partly explained by the high temperatures reached in the vicinity of the electrodes, which might lead to an increase of the drug solubility. Therefore, the produced vapour is capable of transporting more drug, and thus explaining the higher total drug amount in the condensed vapour, compared to the expected values according to its solubility at 25 °C.

On the other hand, as can be seen by the comparison in the Figure 8, the amount of drug transported by the vapours is higher when the nanosuspension-loaded E-liquid is used instead of the raw powder loaded E-liquid, demonstrating the advantage of using nanocrystals. This data not only confirms that ENDS aerosol is able to transport BDP molecules dissolved in the e-vehicle but demonstrates that also suspended BDP (nano)crystals are delivered.

In fact, the analysis of the condensed samples through TEM micrographs prove the presence of drug nanocrystals, as can be seen in the Figure 7c-d, whose morphology and diameter resemble those of the nanocrystals dispersed in the e-liquid (Figure 7a-b).

4. Conclusion

In this study, a BDP nanosuspension was successfully prepared and characterized. The resulting nanocrystals were small in size and homogeneously dispersed, showing an increased solubility compared to the bulk drug. Overall results obtained by the vaping test demonstrated the presence of drug nanocrystals in the produced aerosol. Although we cannot exclude that new particles are formed during the vaporization process, the structural similarity assessed by DLS and TEM suggests that the original BDP nanocrystals were transported by the aerosol. Thus, the ability of ENDS to deliver nanocrystals was confirmed, drawing attention to its possible alternative use as a medical device for poorly soluble drugs.

ENDS have nowadays become common all around the world, due to the proven benefits and less toxicity compared to traditional cigarette smoking (Azzopardi et al., 2016; Czekala et al., 2019). The largest number of adults declare to use ENDS to help them stop smoking (McNeill, A., Brose, L.S., Calder, R., Bauld, L., and Robson, 2020), and a significant part claimed to have satisfactorily stopped (Goniewicz et al., 2013). Therefore, using e-cigarettes with bronchodilators or corticosteroids nanosuspensions – such as BDP – might be advantageous in the treatment of COPD in those patients that are chronic smokers in pursuit of a stop-smoking aid (http://goldcopd.org, 2018). The use of e-cigarette rather than another inhaler device for therapy administration might not only play a key role on the smoking habit cessation, but also ensure better compliance therapy. In fact, patients with chronic respiratory conditions have frequently shown to achieve negative treatment outcomes, linked to inadequate adherence and poor compliance to prescribed therapy (Moroni-Zentgraf, 2013). It is well documented that an effective inhaler technique, which is required to assess an adequate adherence to inhaled medications, is often lacking in many patients, due to scarcity of training or necessary abilities (Ari and Fink, 2011; Nikander, 2010). Hence, owing to the easy operations needed for the activation and the handheld and portable structure, ENDS might represent an inexpensive and simple medical device for the inhalation therapy. All things considered, the eventual regulation of electronic cigarettes as medical device would require an evaluation in terms of quality, safety and efficacy (Boe et al., 2001). Consequently, further studies will be needed to assure the drug delivery potential of the device and the appropriate drug dosing.

Acknowledgements & disclosures

We acknowledge the CeSAR (Centro Servizi Ricerca d'Ateneo) core facility of the University of Cagliari and Dr. Andrea Ardu for assistance with the generation of TEM micrographs.

There is no source of support for this study (grants, gift, equipment or drugs) to declare. The authors are independent from tobacco or electronic cigarette industry and declare no financial relationships with any organizations that might have an interest in the submitted work. In particular, we do not have a source of support to declare from the company that sells the electronic cigarette used in the submitted work.

References

Ari, A., Fink, J.B., 2011. Guidelines for aerosol devices in infants, children and adults: Which to choose, why and how to achieve effective aerosol therapy. Expert Rev. Respir. Med. https://doi.org/10.1586/ers.11.49

Azzopardi, D., Patel, K., Jaunky, T., Santopietro, S., Camacho, O.M., McAughey, J., Gaça, M., 2016. Electronic cigarette aerosol induces significantly less cytotoxicity than Tobacco smoke. Toxicol. Mech. Methods 26, 477–491. https://doi.org/10.1080/15376516.2016.1217112

Boe, J., Dennis, J.H., O'Driscoll, B.R., 2001. European respiratory society guidelines on the use of nebulizers. Eur. Respir. J. 18, 228–242. https://doi.org/10.1183/09031936.01.00220001

Breitbarth, A.K., Morgan, J., Jones, A.L., 2018. E-cigarettes - An unintended illicit drug delivery system. Drug Alcohol Depend. 192, 98–111. https://doi.org/10.1016/j.drugalcdep.2018.07.031

Britland, S., Finter, W., Chrystyn, H., Eagland, D., Abdelrahim, M.E., 2012. Droplet aerodynamics, cellular uptake, and efficacy of a nebulizable corticosteroid nanosuspension are superior to a micronized dosage form. Biotechnol. Prog. 28, 1152–1159. https://doi.org/10.1002/btpr.1616

Brown, C.J., Cheng, J.M., 2014. Electronic cigarettes: Product characterization and design considerations. Tob. Control 23, ii4–ii10. https://doi.org/10.1136/tobaccocontrol-2013-051476

Cheng, T., 2014. Chemical evaluation of electronic cigarettes. Tob. Control 23, ii11–ii17. https://doi.org/10.1136/tobaccocontrol-2013-051482

Chiang, P.C., Alsup, J.W., Lai, Y., Hu, Y., Heyde, B.R., Tung, D., 2009. Evaluation of aerosol delivery of nanosuspension for pre-clinical pulmonary drug delivery. Nanoscale Res. Lett. 4, 254–261. https://doi.org/10.1007/s11671-008-9234-1

Cho, H.J., Balakrishnan, P., Lin, H., Choi, M.K., Kim, D.D., 2012. Application of biopharmaceutics classification system (BCS) in drug transport studies across human respiratory epithelial cell monolayers. J. Pharm. Investig. 42, 147–153. https://doi.org/10.1007/s40005-012-0020-9

Czekala, L., Simms, L., Stevenson, M., Tschierske, N., Maione, A.G., Walele, T., 2019. Toxicological comparison of cigarette smoke and e-cigarette aerosol using a 3D in vitro human respiratory model. Regul. Toxicol. Pharmacol. 103, 314–324. https://doi.org/10.1016/j.yrtph.2019.01.036

De Coster, D.A., Jones, M., Thakrar, N., 2013. Beclometasone for chronic obstructive pulmonary disease. Cochrane Database Syst. Rev. https://doi.org/10.1002/14651858.CD009769.pub2

Dompeling, E., van Schayck, C.P., Molema, J., Folgering, H., van Grunsven, P.M., van Weel, C., 1992. Inhaled beclomethasone improves the course of asthma and COPD. Eur. Respir. J. 5, 945–52.

European Parliament and the Council of the European Union, 2014. Directive 2014/40/EU. Off. J. Eur. Union 127, 1–38.

Giroud, C., de Cesare, M., Berthet, A., Varlet, V., Concha-Lozano, N., Favrat, B., 2015. E-cigarettes: A review of new trends in cannabis use. Int. J. Environ. Res. Public Health 12, 9988–10008. https://doi.org/10.3390/ijerph120809988

Goniewicz, M.L., Gawron, M., Smith, D.M., Peng, M., Jacob, P., Benowitz, N.L., 2017. Exposure to nicotine and selected toxicants in cigarette smokers who switched to electronic cigarettes: A longitudinal within-subjects observational study. Nicotine Tob. Res. 19, 160–167. https://doi.org/10.1093/ntr/ntw160

Goniewicz, M.L., Lingas, E.O., Hajek, P., 2013. Patterns of electronic cigarette use and user beliefs about their safety and benefits: An Internet survey. Drug Alcohol Rev. 32, 133–140. https://doi.org/10.1111/j.1465-3362.2012.00512.x

Goniewicz, M.L., Smith, D.M., Edwards, K.C., Blount, B.C., Caldwell, K.L., Feng, J., Wang, L., Christensen, C., Ambrose, B., Borek, N., van Bemmel, D., Konkel, K., Erives, G., Stanton, C.A., Lambert, E., Kimmel, H.L., Hatsukami, D., Hecht, S.S., Niaura, R.S., Travers, M., Lawrence, C., Hyland, A.J., 2018. Comparison of Nicotine and Toxicant Exposure in Users of Electronic Cigarettes and Combustible Cigarettes. JAMA Netw. open 1, e185937. https://doi.org/10.1001/jamanetworkopen.2018.5937

Hinterwirth, H., Wiedmer, S.K., Moilanen, M., Lehner, A., Allmaier, G., Waitz, T., Lindner, W., Lämmerhofer, M., 2013. Comparative method evaluation for size and size-distribution analysis of gold nanoparticles. J. Sep. Sci. 36, 2952–2961.

https://doi.org/10.1002/jssc.201300460

http://goldcopd.org, 2018. Pocket guide to COPD diagnosis, management and prevention: a guide for health care professionals. https://doi.org/10.2147/copd.2006.1.1.3

Jacobs, C., Müller, R.H., 2002. Production and characterization of a budesonide nanosuspension for pulmonary administration. Pharm. Res. 19, 189–194. https://doi.org/10.1023/A:1014276917363

Lee, D.H., Cho, G.S., Lim, H.M., Kim, D.S., Kim, C., Lee, S.H., 2013. Comparisons of particle size measurement method for colloidal silica. J. Ceram. Process. Res. 14, 274–278.

McNeill, A., Brose, L.S., Calder, R., Bauld, L., and Robson, D., 2020. Vaping in England: an evidence update including mental health and pregnancy, March 2020: a report commissioned by Public Health England., Public Health England (London).

Miliano, C., Scott, E.R., Murdaugh, L.B., Gnatowski, E.R., Faunce, C.L., Anderson, M.S., Reyes, M.M., Gregus, A.M., Buczynski, M.W., 2020. Modeling drug exposure in rodents using e-cigarettes and other electronic nicotine delivery systems. J. Neurosci. Methods. https://doi.org/10.1016/j.jneumeth.2019.108458

Moloughney, J.G., Weisleder, N., 2013. Poloxamer 188 (P188) as a Membrane Resealing Reagent in Biomedical Applications. Recent Pat. Biotechnol. 6, 200–211. https://doi.org/10.2174/1872208311206030200

Moroni-Zentgraf, P., 2013. Impact of Patient Needs on Design and Usage of an Inhalation Device in Respiratory Medicine, in: Respiratory Drug Delivery Europe 2013. pp. 141–152. https://doi.org/10.1586/17476348.1.1.39

Mosharraf, M., Nyström, C., 1995. The effect of particle size and shape on the surface specific dissolution rate of microsized practically insoluble drugs. Int. J. Pharm. 122, 35–47. https://doi.org/10.1016/0378-5173(95)00033-F

Müller, R.H., Peters, K., 1998. Nanosuspensions for the formulation of poorly soluble drugs. I. Preparation by a size-reduction technique. Int. J. Pharm. 160, 229–237. https://doi.org/10.1016/S0378-5173(97)00311-6

Nguyen, J.D., Aarde, S.M., Vandewater, S.A., Grant, Y., Stouffer, D.G., Parsons, L.H., Cole, M., Taffe, M.A., 2016. Inhaled delivery of Δ9-tetrahydrocannabinol (THC) to rats by e-cigarette vapor technology. Neuropharmacology 109, 112–120.

https://doi.org/10.1016/j.neuropharm.2016.05.021

Nikander, K., 2010. Challenges and opportunities in respiratory drug delivery devices. Expert Opin. Drug Deliv. https://doi.org/10.1517/17425247.2010.525231

Pabisch, S., Feichtenschlager, B., Kickelbick, G., Peterlik, H., 2012. Effect of interparticle interactions on size determination of zirconia and silica based systems - A comparison of SAXS, DLS, BET, XRD and TEM. Chem. Phys. Lett. 521, 91–97. https://doi.org/10.1016/j.cplett.2011.11.049

Patravale, V.B., Date, A.A., Kulkarni, R.M., 2004. Nanosuspensions: a promising drug delivery strategy. J. Pharm. Pharmacol. 56, 827–840. https://doi.org/10.1211/0022357023691

Pourchez, J., de Oliveira, F., Perinel-Ragey, S., Basset, T., Vergnon, J.M., Prévôt, N., 2017. Assessment of new-generation high-power electronic nicotine delivery system as thermal aerosol generation device for inhaled bronchodilators. Int. J. Pharm. 518, 264–269. https://doi.org/10.1016/j.ijpharm.2017.01.009

Round, E.K., Chen, P., Taylor, A.K., Schmidt, E., 2019. Biomarkers of Tobacco Exposure Decrease After Smokers Switch to an E-Cigarette or Nicotine Gum. Nicotine Tob. Res. 21, 1239–1247. https://doi.org/10.1093/ntr/nty140

Tomaszewska, E., Soliwoda, K., Kadziola, K., Tkacz-Szczesna, B., Celichowski, G., Cichomski, M., Szmaja, W., Grobelny, J., 2013. Detection limits of DLS and UV-Vis spectroscopy in characterization of polydisperse nanoparticles colloids. J. Nanomater. 2013, 1–10. https://doi.org/10.1155/2013/313081

Trtchounian, A., Williams, M., Talbot, P., 2010. Conventional and electronic cigarettes (e-cigarettes) have different smoking characteristics. Nicotine Tob. Res. 12, 905–912. https://doi.org/10.1093/ntr/ntq114

Tscharnuter, W., 2006. Photon Correlation Spectroscopy in Particle Sizing. Encycl. Anal. Chem. 1–16. https://doi.org/10.1002/9780470027318.a1512

Unsoy, G., Yalcin, S., Khodadust, R., Gunduz, G., Gunduz, U., 2012. Synthesis optimization and characterization of chitosancoated iron oxide nanoparticles produced for biomedical applications. J. Nanoparticle Res. 14, 1–13. https://doi.org/10.1007/s11051-012-0964-8

Van Eerdenbrugh, B., Van den Mooter, G., Augustijns, P., 2008. Top-down production of drug nanocrystals: Nanosuspension stabilization, miniaturization and transformation into solid

products. Int. J. Pharm. https://doi.org/10.1016/j.ijpharm.2008.07.023

Varlet, V., 2016. Drug Vaping: From the Dangers of Misuse to New Therapeutic Devices. Toxics 4, 29. https://doi.org/10.3390/toxics4040029

Varlet, V., Concha-Lozano, N., Berthet, A., Plateel, G., Favrat, B., De Cesare, M., Lauer, E., Augsburger, M., Thomas, A., Giroud, C., 2016. Drug vaping applied to cannabis: Is "cannavaping" a therapeutic alternative to marijuana. Sci. Rep. 6, 1–13. https://doi.org/10.1038/srep25599

Wang, Z., Chen, J.F., Le, Y., Shen, Z.G., Yun, J., 2007. Preparation of ultrafine beclomethasone dipropionate drug powder by antisolvent precipitation. Ind. Eng. Chem. Res. 46, 4839–4845. https://doi.org/10.1021/ie0615537

Wauthoz, N., Amighi, K., 2015. Formulation Strategies for Pulmonary Delivery of Poorly Soluble Drugs, in: Pulmonary Drug Delivery. John Wiley & Sons, Ltd, pp. 87–122. https://doi.org/10.1002/9781118799536.ch5

Weiss, C., McLoughlin, P., Manesiotis, P., Redington, W., Cathcart, H., 2018. Preparation and characterization of beclomethasone dipropionate solvates. Cryst. Growth Des. 18, 5832–5844. https://doi.org/10.1021/acs.cgd.8b00465

Williams, M., Villarreal, A., Bozhilov, K., Lin, S., Talbot, P., 2013. Metal and Silicate Particles Including Nanoparticles Are Present in Electronic Cigarette Cartomizer Fluid and Aerosol. PLoS One 8, 1–11. https://doi.org/10.1371/journal.pone.0057987

Wood, A.J. j., Barnes, P.J., 1995. Inhaled glucocorticoids for asthma. N. Engl. J. Med. https://doi.org/10.1056/NEJM199503303321307

Yang, J.Z., Young, A.L., Chiang, P.C., Thurston, A., Pretzer, D.K., 2008. Fluticasone and budesonide nanosuspensions for pulmonary delivery: Preparation, characterization, and pharmacokinetic studies. J. Pharm. Sci. 97, 4869–4878. https://doi.org/10.1002/jps.21380

Zhang, Y., Zhang, J., 2016. Preparation of budesonide nanosuspensions for pulmonary delivery: Characterization, in vitro release and in vivo lung distribution studies. Artif. Cells, Nanomedicine Biotechnol. 44, 285–289. https://doi.org/10.3109/21691401.2014.944645